

Optimized Design Study of Black Pottery Forward and Reverse Knife Carving Tools

Mu Bo^{1,2}, Mohammad Puad Bebit ^{2*}, Addley Bromeo Bianus², Sun Xuejie¹

¹School of Art and Design, Wuhan Institute of Technology, China

²Academy of Arts and Creative Technology, Universiti Malaysia Sabah, Malaysia

* Corresponding Author

DOI: <https://dx.doi.org/10.47772/IJRISS.2025.91100230>

Received: 21 November 2025; Accepted: 28 November 2025; Published: 05 December 2025

ABSTRACT

The forward and reverse knife technique is the core method used in black pottery carving, yet traditional carving tools are mostly handcrafted by artisans using improvised materials, often resulting in poor ergonomics and low efficiency. To address these issues, this study develops an improved carving tool aimed at enhancing both comfort and productivity. A pressure-based reverse engineering experiment was conducted to analyze the distribution of hand pressure during carving, providing quantitative data for ergonomic optimization. Based on the operational requirements of the forward and reverse knife techniques and the habitual postures of artisans, the handle's curvature and grip form were refined to better fit the natural contours of the hand. The optimized handle effectively distributes and alleviates pressure on the palm and fingers during prolonged use, minimizing fatigue and reducing the risk of hand strain. Overall, the improved tool design not only enhances carving efficiency and operational stability but also contributes to the sustainable protection of artisans' hand health, offering a practical reference for ergonomic tool innovation in traditional handicrafts.

Keywords: Black pottery, carving tools, design, forward and reverse knife

INTRODUCTION

Black pottery, as a shining pearl in the history of human creation, plays a pivotal role in the field of ceramic art with its exquisite carving and hollowing techniques (Colomban, 2020). It represents not only a technical achievement but also a profound cultural expression that reflects the harmony between craftsmanship, material, and aesthetic philosophy (Chinyana, 2017). Among the many artistic methods of black pottery decoration, the classic carving technique—known as the forward and reverse knife method—stands out for its precision and expressive power (Vickers, 1985). This method requires years of accumulated experience and delicate control, as it integrates both the strength of cutting and the subtlety of shaping into a seamless artistic process (Yussif et al., 2018).

This forward and reverse knife technique involves the alternate use of the front and back of the blade to finely cut, engrave, and shape the clay body before firing. The rhythm of movement is crucial: the forward knife cuts lightly and straight, while the reverse knife moves obliquely and deeply; then, the forward knife shifts into a deeper, slanted motion, and the reverse knife returns shallow and straight. Through this repeated alternation, the artisan produces an intricate, dynamic surface that embodies the unique aesthetic and tactile appeal of black pottery carving. This process demands both physical endurance and refined motor control, as even slight deviations can affect the quality and symmetry of the final work.

In the traditional production process, black pottery artisans tend to rely on self-made carving tools, often created from readily available materials such as iron sheets, spring steel plates, or other metal fragments (Buchczyk, 2015). The blade's length and shape directly determine its purpose: short blades are used for fine, detailed engraving, while longer blades are suited for hollowing, trimming, and shaping tasks. Over generations of

practice, artisans have developed various personalized tool modifications to improve their functionality. Despite their humble appearance, these tools embody the ingenuity and adaptive creativity of craftsmen, who continuously refine them based on tactile feedback and work habits.

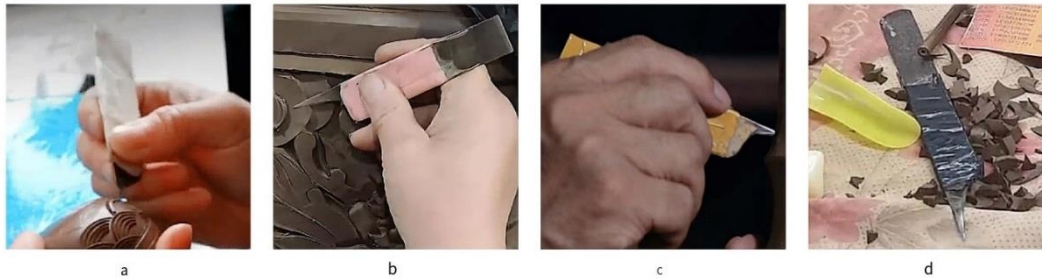


Figure 1: Traditional black pottery carving knife

To enhance safety and usability, craftsmen have traditionally wrapped the midsection and rear end of the metal sheet with layers of cloth, paper, or adhesive tape, forming a simple handle that increases friction and reduces the direct pressure of metal against skin. This practical adaptation allows artisans to maintain grip stability and control while reducing the immediate risk of hand injury during long carving sessions (Figure 1). However, such temporary ergonomic solutions remain far from ideal. The flat, narrow shape of the improvised handle leads to uneven pressure distribution, causing excessive strain on the fingers and palm during repetitive use. Over time, this results in localized hand pain, blisters, or even chronic fatigue symptoms that compromise both comfort and precision.

Moreover, the carving process in black pottery production is highly time-consuming and physically demanding. Artisans must sustain precise, repetitive hand movements for several hours at a time, maintaining consistent control of tool angle and depth. Under these prolonged working conditions, the lack of ergonomic support significantly increases muscular tension and operational resistance, making the process more tiring and less efficient. The accumulation of such strain not only affects artisans' physical health but also limits their ability to maintain high-quality craftsmanship in the long term.

To address these ergonomic deficiencies, this study aims to develop an optimized black pottery carving tool that integrates principles of human-machine interaction design with traditional craftsmanship. Specifically, a pressure-based reverse engineering method is employed to analyze the distribution of hand pressure when using conventional carving tools. Through experimental testing and mapping, the study identifies key stress points and contact areas, providing scientific data to guide ergonomic optimization.

Based on the results, a new handle design is proposed that adapts to the natural curvature of the artisan's hand, balancing pressure and improving comfort. The optimized handle features a smoother curvature, wider side surfaces, and an enhanced grip texture, allowing for a more even distribution of force across the palm and fingers. This effectively reduces localized stress, minimizes fatigue, and enhances operational stability during prolonged carving sessions. Furthermore, the improved handle design not only reduces physical discomfort but also enhances precision, control, and efficiency in carving. By allowing the tool to conform more naturally to the user's hand movements, it facilitates a smoother and more continuous workflow, improving both the speed and quality of black pottery production.

The significance of this research lies not only in improving tool usability but also in promoting the modernization of traditional craftsmanship through ergonomic innovation. By integrating scientific analysis with artisanal experience, the study provides a new approach for the sustainable development and preservation of intangible cultural heritage techniques. The ergonomic design of carving tools contributes to protecting artisans' health, extending their creative lifespan, and ensuring the consistent transmission of traditional craftsmanship.

MATERIALS AND METHOD

Overview of Pressure-Based Reverse Engineering Principles in Ergonomics

In the design optimization of handheld tools, the handle plays a pivotal role in enhancing ergonomic performance. By refining the shape of the tool grip and optimizing the curvature of the handle surface, the pressure distribution on the hand can be effectively dispersed, thereby reducing localized pressure concentration and significantly improving user comfort. This design philosophy reflects not only meticulous attention to detail but also a profound commitment to user experience (Hassenzahl, 2013). Reverse Engineering (RE) focuses on utilizing precise measurement devices to conduct comprehensive scans of physical objects or models, followed by reconstructing 3D digital models using advanced geometric modeling techniques (Bhaskaran, 2024). This process transforms physical samples into digital information models, laying a foundation for subsequent product design and manufacturing. Building on this, pressure-based reverse engineering introduces an innovative approach: it designs and optimizes the handle's surface curvature based on the morphological changes of the human hand under pressure, aiming to achieve superior ergonomic alignment and comfort.

To improve the efficiency and comfort of the forward and reverse knife technique during black pottery engraving, this study leverages pressure-based reverse engineering experiments and operational characteristics of the technique to design a specialized handle for black pottery carving tools. The prototype was evaluated by artisans to collect feedback, guiding further optimization for a second-generation design (Burden, 2022).

Model Principles and Parameter Sources

Hand Anatomy and Function

As the primary interface for tool operation, the hand's structure and functionality are critical to handle design. The hand, a complex and highly organized organ, comprises bones, nerves, muscles, skin, and blood vessels. It enables not only basic gripping but also intricate actions like lifting and twisting. The human body contains 206 bones, 54 of which are in the hands and wrists—nearly a quarter of the total. A single hand and wrist consist of 27 bones, categorized into three groups: 5 metacarpal bones, 8 carpal bones, and 14 phalanges (Figure 2). During gripping, muscles in the forearm and hand contract, transmitting force through tendons to bones, while ligaments connect adjacent bones.

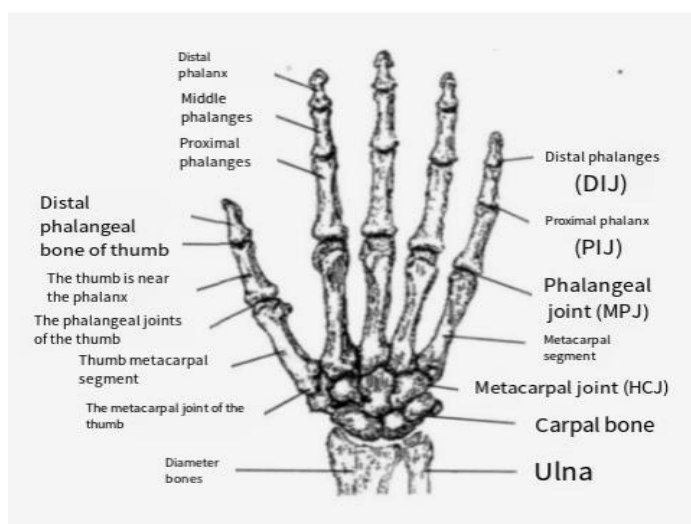


Figure 2: Anatomical structure of the human hand

Hand joints exhibit diverse motions, including extension, lateral deviation, and flexion. Lateral deviation primarily occurs at the metacarpophalangeal joints, while flexion and extension involve coordination between the proximal interphalangeal, metacarpophalangeal, and distal interphalangeal joints. Extension relies on muscles like the lumbricals, dorsal interossei, and extensor digitorum, whereas flexion engages the lumbricals, flexor digitorum profundus, and flexor digitorum superficialis.

Hand Posture Data During Black Pottery Carving

Field research identified two primary hand postures during black pottery carving: pen-holding posture and handle-holding posture (Figures 3 and 4). The pen-holding posture is more prevalent due to its versatility in detailed engraving and prolonged use. In practice, six critical contact points exist between the carving knife and the hand (Figure 5).

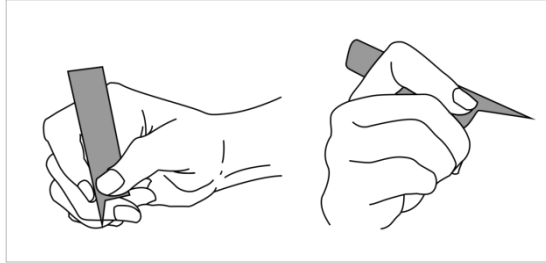


Figure 3: Traditional carving knife holding posture 1

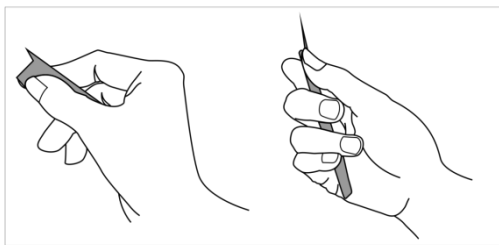


Figure 4: Traditional carving knife holding Posture 2

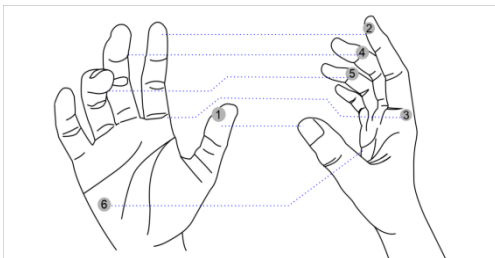


Figure 5: Traditional carving knife holding posture - handle style

As a finger-operated tool, the carving knife primarily interacts with the thenar and hypothenar eminences, supported by muscles in the palm and forearm. Thus, ergonomic improvements must address three key factors: (1) Anatomical compatibility: the limited contact area between the knife and hand necessitates strict adherence to hand anatomy to reduce localized pressure on the thenar eminence. The grip surface should be smooth to avoid skin irritation while incorporating subtle textures or friction-enhancing materials (e.g., rubber or finely grooved surfaces) to ensure stability without compromising comfort; (2) Balanced weight distribution: excessive weight causes fatigue during prolonged use, while insufficient weight increases operational effort. Imbalanced weight distribution between the thumb and index finger (as pivot points) may destabilize the tool, posing safety risks. Optimal weight design requires careful material selection and structural engineering; (3) Hygienic design: in dusty pottery environments, the handle should feature a simple, easy-to-clean structure to prevent clay buildup and maintain hygiene.

Experimental process

Determination of Basic Handle Types and Questionnaire Reliability

(1) Basic Handle Design

When designing the finger-contact portion of the tool, elliptical or circular cross-sectional shapes are preferred (Basak, 2007; Gardner & Chan, 2007). Based on the previously described pen-holding posture for the forward and reverse knife technique, and referencing commercially available handle designs, six cylindrical handle prototypes were created. For rigorous comparative analysis, the original thin rectangular handle of the carving knife was retained, resulting in seven distinct basic handle types.

Table 1: Basic dimensions of handle with torque handwheel and steering handle

Maneuvering mode	Handle diameter d		Handle length L	
	Size range	Preferred choice	Size range	preference
Hand grip handle	15 ~ 35	25 ~ 30	75 ~ 150	100 ~ 120
Finger handshake handle	10 ~ 520	12 ~ 18	30 ~ 75	45 ~ 50

Table 2: Basic dimensions of joystick shank

Shank shape	Diameter d				Handle length L			
	Finger grip		Hand grip		Finger grip		Hand grip	
	Size range	Preferred choice	Size range	Preferred choice	Size range	Preferred choice	Size range	Preferred choice
Spherical, pear-shaped, tapered	10 ~ 40	30	35 ~ 50	40	15 ~ 60	40	40 ~ 60	50
Spindle shape, cylinder shape	10 ~ 30	20	20 ~ 40	28	30 ~ 90	60	80 ~ 130	100

All prototypes were fabricated using industrial modeling clay with a hardness of 25 to ensure testing consistency. Thirty participants of varying heights, genders, and hand sizes were invited to evaluate the prototypes. Each participant simulated black pottery carving motions while holding all seven handle types and rated their comfort and usability. This test aimed to investigate how handle shapes influence carving comfort and efficiency, providing critical data for subsequent design optimization.

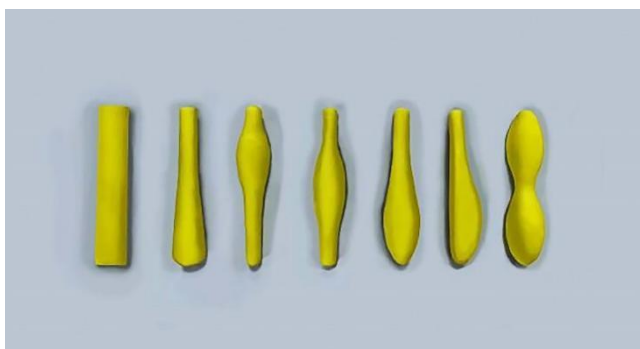


Figure 6: Handle base model

Questionnaire Reliability Testing

Reliability, defined as the consistency and stability of measurement results, evaluates whether a tool accurately captures its intended targets. Internal consistency reliability assesses correlations between questionnaire items (Can and Ling, 2008). For a questionnaire with k items, Cronbach's α coefficient is calculated as:

$$\alpha = \frac{k}{k-1} \left(1 - \frac{\sum_{i=1}^k s_i^2}{s_T^2} \right)$$

where S_i^2 is the variance of the i -th item's scores, and S_T^2 is the variance of the total scores. This coefficient reflects internal consistency among items, equivalent to the average of all possible split-half reliability coefficients. For multi-domain questionnaires, α should be calculated per domain to avoid reduced consistency. A Cronbach's $\alpha \geq 0.80$ indicates good reliability. The test questionnaire included seven mandatory multiple-choice questions (1–5 Likert scale: 1 = "very dissatisfied," 5 = "very satisfied") and one optional open-ended question for design feedback. With $k=7$, the calculated α coefficient was approximately 0.93, confirming high reliability and measurement stability.

Carving knife handle comfort evaluation questionnaire

Hello! Thank you very much for taking time out of your busy schedule to participate in our survey. This questionnaire is divided into two parts, the first part is personal information; The second part includes the comfort rating of simulated carving.

The information you fill in is very important to us, this information is only for academic research and will not be made public, so please do not have any concerns. Thank you very much for your help!








I. Personal Information:

Gender:

Height:

2. Assessment content:

According to your simulated experience of carving black pottery, please rate the comfort feeling of the following six different shapes of the carving knife handle. The greater the score, the higher the comfort level. ① Round table knife handle:

	Very uncomfortable	1	2	3	4	5	Very comfortable
② Upper elliptical knife handle:	Very uncomfortable	1	2	3	4	5	Very comfortable
	Very uncomfortable	1	2	3	4	5	Very comfortable
③ Medium oval knife handle:	Very uncomfortable	1	2	3	4	5	Very comfortable
	Very uncomfortable	1	2	3	4	5	Very comfortable
④ Lower oval knife handle:	Very uncomfortable	1	2	3	4	5	Very comfortable
	Very uncomfortable	1	2	3	4	5	Very comfortable
⑤ Half oval knife handle:	Very uncomfortable	1	2	3	4	5	Very comfortable
	Very uncomfortable	1	2	3	4	5	Very comfortable
⑥ 8-figure knife handle:	Very uncomfortable	1	2	3	4	5	Very comfortable
	Very uncomfortable	1	2	3	4	5	Very comfortable
⑦ Slice type knife handle:	Very uncomfortable	1	2	3	4	5	Very comfortable
	Very uncomfortable	1	2	3	4	5	Very comfortable

Additional comments (optional) :

Please provide any additional comments, suggestions, or ideas for improving the handle design below:

Figure 7: Basic model evaluation questionnaire

Questionnaire Results and Final Basic Type Selection

All 30 participants completed the mandatory questions (100% response rate), while the optional open-ended question had a 6.7% response rate. Analysis of handle type preferences revealed the following rankings: Semi-elliptical type: 21.74%, Flat type: 15.15%, Medium-elliptical type: 14.76%, Lower-elliptical type: 13.79%, Upper-elliptical type: 13.61%, Truncated cone type: 10.95%, Figure-8 type: 9.99%.

Table 3: Results of the questionnaire

Items	Questionnaire Participants	Score						
		①	②	③	④	⑤	⑥	⑦
1	Wang ¹	1	2	3	2	5	2	2
2	Zhang ¹	2	3	4	1	4	1	3
3	Wan	2	3	3	2	4	2	4
4	Chen ¹	1	2	3	2	3	1	3
5	Hu	2	2	3	3	4	2	3
6	Li ¹	2	2	2	3	5	3	2
7	Zhao ¹	3	3	3	3	4	2	2
8	Zhen	2	4	3	3	4	1	3
9	Guo	2	2	2	2	3	2	4
10	Xu	1	2	2	3	3	3	3
11	Mu	2	4	3	4	4	1	2
12	Han ¹	4	2	3	3	5	2	3
13	Wang ²	1	1	3	2	4	2	2
14	Li ²	2	2	3	1	4	2	2
15	Zong	2	2	3	3	5	2	3
16	Zhang ²	2	3	2	5	4	2	3
17	Han ²	2	2	2	3	4	2	4
18	Liu	2	2	3	2	2	1	2
19	Xia	2	3	3	2	4	1	3
20	Zhang ³	1	2	3	2	3	2	2
21	Chen ²	1	2	3	2	3	3	3
22	Wang ³	1	3	2	2	3	2	2
23	Zhang ⁴	2	2	2	1	5	3	3
24	Yang	1	2	1	4	3	2	3
25	Zeng	4	3	2	1	4	1	2
26	Zhao ²	2	2	3	3	4	1	3
27	Yuan	2	2	2	2	3	1	2
28	Li ³	3	4	3	2	4	2	2
29	Cui	2	2	3	3	4	1	3
30	He	2	2	1	2	4	1	2

Table 4: Distribution of base model scores

Basic Model Categories	Average Score	Percentage of the score	
Round table knife handle	1.93	<div><div></div></div>	10.95%
Put on the elliptical handle	2.4	<div><div></div></div>	13.61%
Middle oval handle	2.6	<div><div></div></div>	14.76%
Lower oval handle	2.43	<div><div></div></div>	13.79%
Semi-oval handle	3.83	<div><div></div></div>	21.74%
8 Font handle	1.76	<div><div></div></div>	9.99%
Blade handle	2.67	<div><div></div></div>	15.15%

Given its dominant performance, the semi-elliptical type was selected as the foundational model for subsequent experiments, offering unique insights into ergonomic optimization.

Master Mold Preparation and Mass-Produced Clay Models

In silicone mold casting, the inner surface smoothness critically impacts final product quality. To address this, a high-smoothness PLA material was 3D-printed to replicate the semi-elliptical handle's geometry, ensuring precision and stability during silicone encapsulation. A 35-degree milky-white silicone (Hengxin brand) was poured twice to create the master mold. Soft modeling clay (hardness 25) was used as a support medium. The PLA sub-mold was partially embedded in clay, with vents and gates formed using cylindrical rods. The first silicone pour was conducted in a sealed container and cured for 24 hours. A 5mm-thick gypsum layer (gypsum-to-water ratio 1:2) was applied to reinforce the silicone mold. After gypsum solidification, a second silicone pour ensured full encapsulation of the sub-mold, yielding a high-precision master mold with excellent surface finish.

Thermoplastic modeling clay (temperature-sensitive) was injected into the silicone master mold. This material exhibits ideal plasticity near body temperature ($\approx 37^{\circ}\text{C}$), making it suitable for hand-motion simulations. After curing, multiple clay prototypes were extracted for experimental use.

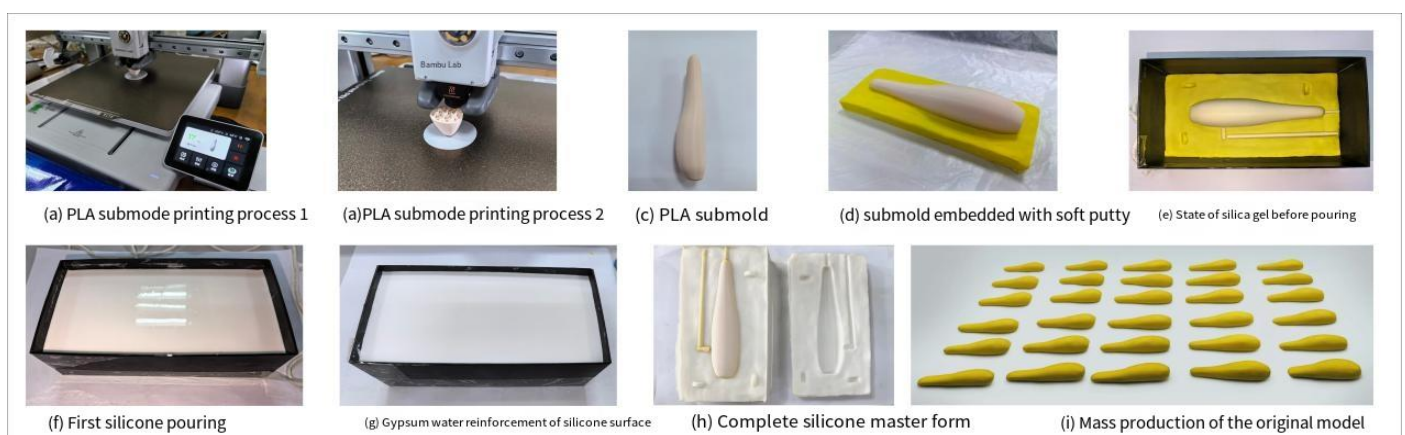


Figure 8: Preparation of basic master mold and mass production sludge model

Acquisition and Preservation of Scanned Models

To collect comprehensive and representative experimental data, 30 participants with varying hand sizes and ages were invited. Each participant simulated the pen-holding posture used in black pottery carving with the forward and reverse knife technique, adjusting the thermoplastic clay prototype to their optimal grip and comfort. During

the process, four primary contact points between the hand and clay model were recorded and marked with red ink for subsequent analysis and optimization. After shaping, the clay models were carefully removed and preserved at low temperatures to minimize thermal deformation, ensuring data accuracy. This rigorous protocol yielded 30 preserved clay models for subsequent scanning.

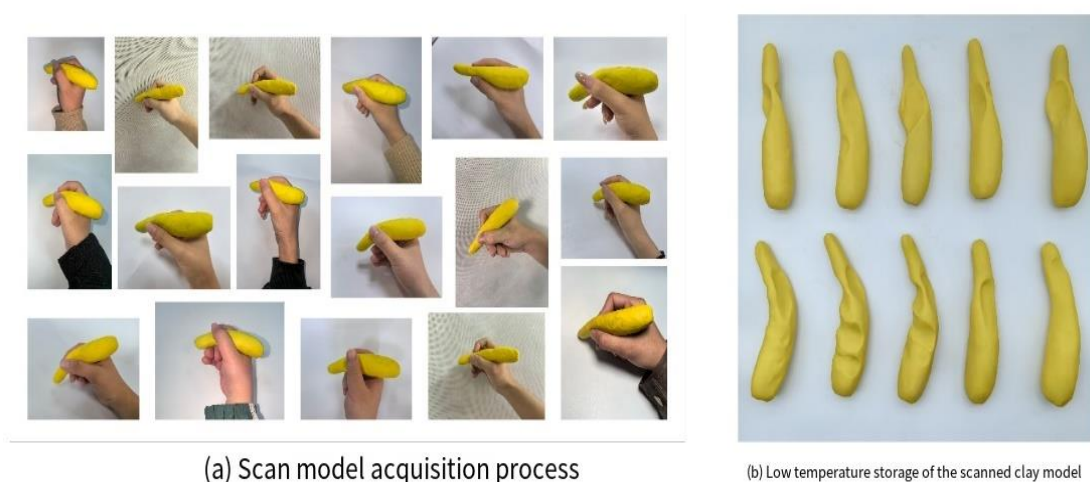


Figure 9: Process of obtaining scanned part model and preservation of sludge model

Experimental Data Acquisition

The ZGScan handheld 3D scanner was employed for measurements (Jędrych et al., 2025; Pätöprstý et al., 2024). Its core technology utilizes white-light grating fringe projection for high-precision surface scanning. The scanner projects controlled laser stripes onto the object, which deform according to surface geometry. A pre-calibrated camera system captures and analyzes these deformations to extract linear 3D coordinates. The scanner moves, it continuously records 3D coordinates of laser-covered areas, ensuring data consistency through real-time spatial positioning. Advanced algorithms process these dynamic coordinates to reconstruct surface geometry and texture. The resulting 3D data and texture maps are imported into Art Mapping, a point-cloud and image registration system. This software aligns discrete point clouds with texture images, generating high-fidelity 3D models for quantitative analysis and morphological comparisons.

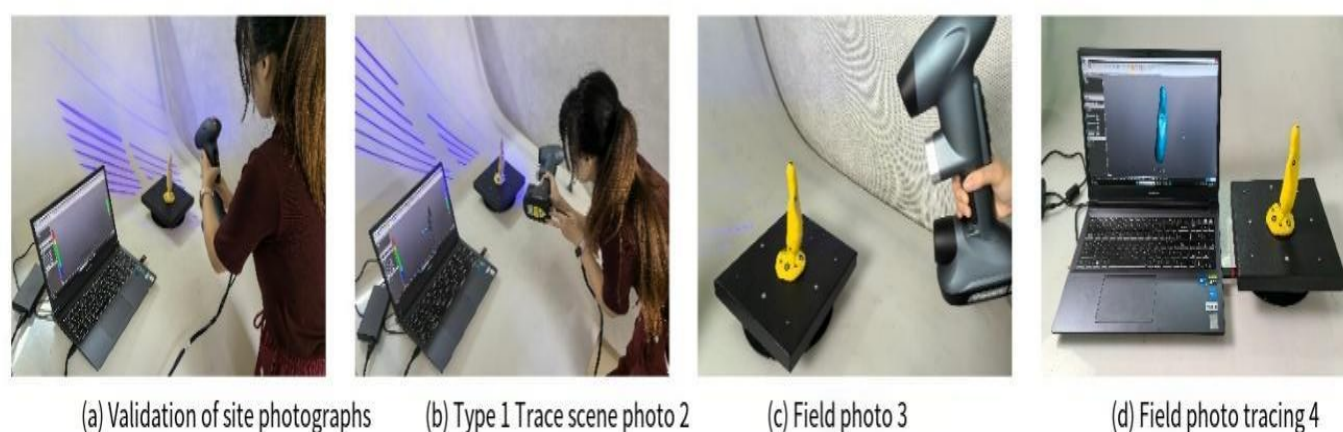


Figure 10: canning the site

3D models of all 30 samples were acquired. To standardize analysis, the center point of each model's widest diameter (least-deformed region) was defined as the reference origin, with its vertical axis as the reference axis. Models were aligned in a virtual space, ensuring their origins coincided and axes aligned perpendicular to the z-axis.

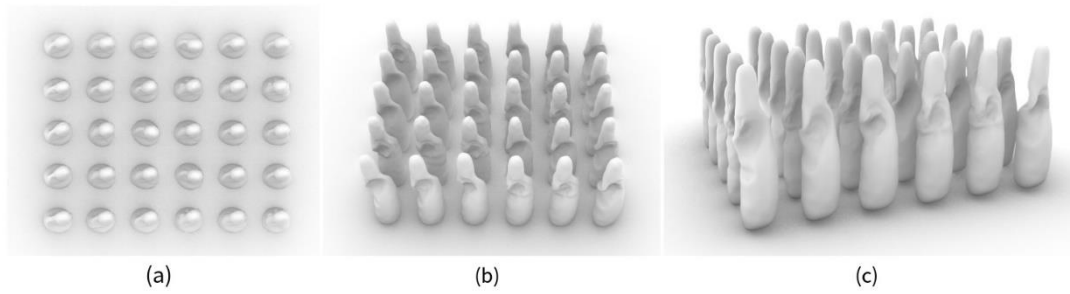


Figure 11: Experimental results 3D model

For each model, spatial coordinates of the four contact points were recorded. Horizontal cross-sectional profiles at these points were extracted, yielding four sets of profile lines.

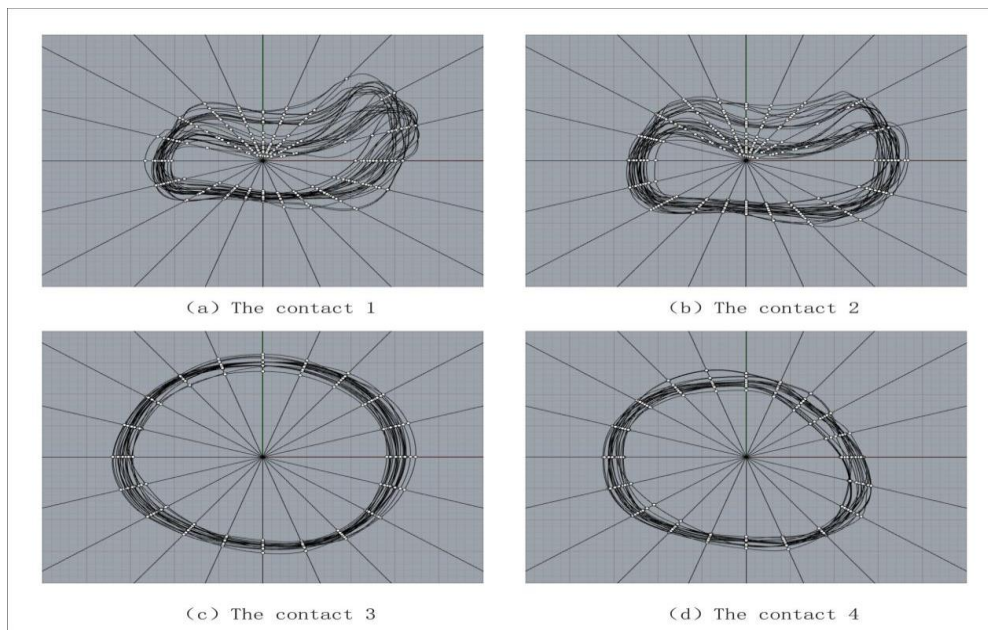


Figure 12: Profile line where the contact is located

To analyze these profiles, 20 radial lines (labeled Line1–Line20) were drawn from the origin, intersecting all 30 cross-sectional profiles. The x and y coordinates of intersection points were measured, and median coordinates for each line were calculated using:

$$(x_i, y_i) = \left(\frac{\sum_{j=1}^{30} x_{ij}}{30}, \frac{\sum_{j=1}^{30} y_{ij}}{30} \right)$$

Where, (x_i, y_i) represents the coordinates of the middle point on Line i, x_{ij}, y_{ij} respectively represents the abscissa and ordinate of the intersection point between Line i and the J-section line. Connecting these median points generated median path lines for each contact point's horizontal profile.

Table 5: Midpoint coordinates of the first contact

Contact one	Slope K	Mean point coordinates X	Mean point coordinates Y	Median point coordinates
line1	-0.32	-3.54	10.88	10.88, 3.54, 75.27

line2	-0.73	-5.29	7.28	7.28, 5.29, 75.27
line3	-1.38	-5.65	4.10	4.1, 5.65, 75.27
line4	-3.08	-5.73	1.86	1.86, 5.73, 75.27
line5	0	-5.61	0	0, 5.61, 75.27
line6	3.08	-5.38	-1.75	1.75, 5.38, 75.27
line7	1.38	-5.11	-3.71	3.71, 5.11, 75.27
line8	0.73	-4.96	-6.82	6.82, 4.96, 75.27
line9	0.32	-3.53	-10.86	10.86, 3.53, 75.27
line10	0	0	-11.56	11.56, 0, 75.27
line11	-0.32	3.28	-10.11	10.11, 3.28, 75.27
line12	-0.73	4.77	-6.56	6.56, 4.77, 75.27
line13	-1.38	4.83	-3.51	3.51, 4.83, 75.27
line14	-3.08	4.35	-1.41	1.41, 4.35, 75.27
line15	0	4.03	0	0, 4.03, 75.27
line16	3.08	3.96	1.29	1.29, 3.96, 75.27
line17	1.38	4.31	3.13	3.13, 4.31, 75.27
line18	0.73	5.51	8.11	8.11, 5.51, 75.27
line19	0.32	4.17	12.83	12.83, 4.17, 75.27
line20	0	0	13.64	13.64, 0, 75.27

Table 6: Midpoint coordinates of the second contact

Contact two	Slope K	Mean point X coordinates	Mean point Y coordinates	Median point coordinates
line1	-0.32	14.89	-4.84	14.89, 4.84, 81.09
line2	-0.73	10.62	-7.72	10.62, 7.72, 81.09
line3	-1.38	5.93	-8.16	5.93, 8.16, 81.09
line4	-3.08	2.54	-7.83	2.54, 7.83, 81.09
line5	0	0	-7.50	0, 7.5, 81.09
line6	3.08	-2.37	-7.29	2.37, 7.29, 81.09

line7	1.38	-5.26	-7.24	5.26, 7.24, 81.09
line8	0.73	-9.35	-5.65	9.35, 5.65, 81.09
line9	0.32	-11.98	-3.89	11.98, 3.89, 81.09
line10	0	-12.24	0	12.24, 0,81.09
line11	-0.32	-10.91	3.54	10.91, 3.54, 81.09
line12	-0.73	-7.71	5.60	7.71, 5.6, 81.09
line13	-1.38	-3.99	5.50	3.99, 5.5, 81.09
line14	-3.08	-1.50	4.63	1.5, 4.63, 81.09
line15	0	0	4.10	0,4.1, 81.09
line16	3.08	1.24	3.82	1.24, 3.82, 81.09
line17	1.38	2.79	3.83	2.79, 3.83, 81.09
line18	0.73	6.33	4.60	6.33, 4.6, 81.09
line19	0.32	12.03	3.91	12.03, 3.91, 81.09
line20	0	16.49	0	16.49, 0,81.09

Table 7: Midpoint coordinates of the third contact

Contact three	Slope K	Mean point X coordinate	Mean point Y coordinates	Median point coordinates
line1	-0.32	14.51	-4.71	14.51, 4.71, 25.81
line2	-0.73	12.38	-8.99	12.38, 8.99, 25.81
line3	-1.38	8.94	-12.31	8.94, 12.31, 25.81
line4	-3.08	4.56	-14.02	4.56, 14.02, 25.81
line5	0	0	-14.15	0, 14.15, 25.81
line6	3.08	-4.33	-13.32	4.33, 13.32, 25.81
line7	1.38	-8.39	-11.55	8.39, 11.55, 25.81
line8	0.73	-12.14	-8.82	12.14, 8.82, 25.81
line9	0.32	-14.81	-4.81	14.81, 4.81, 25.81
line10	0	-15.76	0	15.76, 0,25.81
line11	-0.32	-14.79	4.81	14.79, 4.81, 25.81

line12	-0.73	-12.56	9.13	12.56, 9.13, 25.81
line13	-1.38	-9.09	12.52	9.09, 12.52, 25.81
line14	-3.08	-4.70	14.47	4.7, 14.47, 25.81
line15	0	0	15.07	0,15.07, 25.81
line16	3.08	4.68	14.41	4.68, 14.41, 25.81
line17	1.38	9.00	12.39	9,12.39, 25.81
line18	0.73	12.57	9.13	12.57, 9.13, 25.81
line19	0.32	14.79	4.81	14.79, 4.81, 25.81
line20	0	15.45	0	15.45, 0,25.81

Table 8: The coordinates of the middle point of the fourth contact

Contact four	Slope K	Mean point X coordinates	Mean point Y coordinates	Median point coordinates
line1	-0.32	12.98	-4.22	12.98, 4.22, 56.43
line2	-0.73	11.85	-8.61	11.85, 8.61, 56.43
line3	-1.38	8.71	-11.99	8.71, 11.99, 56.43
line4	-3.08	4.43	-13.64	4.43, 13.64, 56.43
line5	0	0	-13.55	0, 13.55, 56.43
line6	3.08	-4.16	-12.79	4.16, 12.79, 56.43
line7	1.38	-8.18	-11.27	8.18, 11.27, 56.43
line8	0.73	-11.94	-8.68	11.94, 8.68, 56.43
line9	0.32	-14.31	-4.65	14.31, 4.65, 56.43
line10	0	-15.05	0	15.05, 0,56.43
line11	-0.32	-14.25	4.63	14.25, 4.63, 56.43
line12	-0.73	-11.69	8.49	11.69, 8.49, 56.43
line13	-1.38	-7.90	10.88	7.9, 10.88, 56.43
line14	-3.08	-3.83	11.78	3.83, 11.78, 56.43
line15	0	0	11.95	0,11.95, 56.43
line16	3.08	3.55	10.92	3.55, 10.92, 56.43

line17	1.38	6.31	8.69	6.31, 8.69, 56.43
line18	0.73	8.60	6.25	8.6, 6.25, 56.43
line19	0.32	10.59	3.44	10.59, 3.44, 56.43
line20	0	12.22	0	12.22, 0,56.43

Experimental Conclusions

Among the four median horizontal profile lines, the median path lines corresponding to Contact Points 1 and 2 exhibited the most significant deformation characteristics, strongly indicating these areas were subjected to the highest pressure concentrations. In contrast, the median path line of Contact Point 3 closely approximated an ideal circle with negligible deformation. This stability can be attributed to two factors: Orientation and Load Distribution: Contact Point 3 faces downward, positioned precisely on the surface of the metacarpophalangeal joint of the index finger. Its mechanical state remains stable due to the combined load of the thermoplastic clay model's self-weight and the supportive force from the joint surface, minimizing deformation. For Contact Point 4, the median path line displayed a distinct collapse in its upper-right segment, clearly reflecting substantial pressure from the distal phalanx and interphalangeal joint surface of the middle finger. This deformation confirms the critical role of the middle finger in generating localized compressive forces during carving.

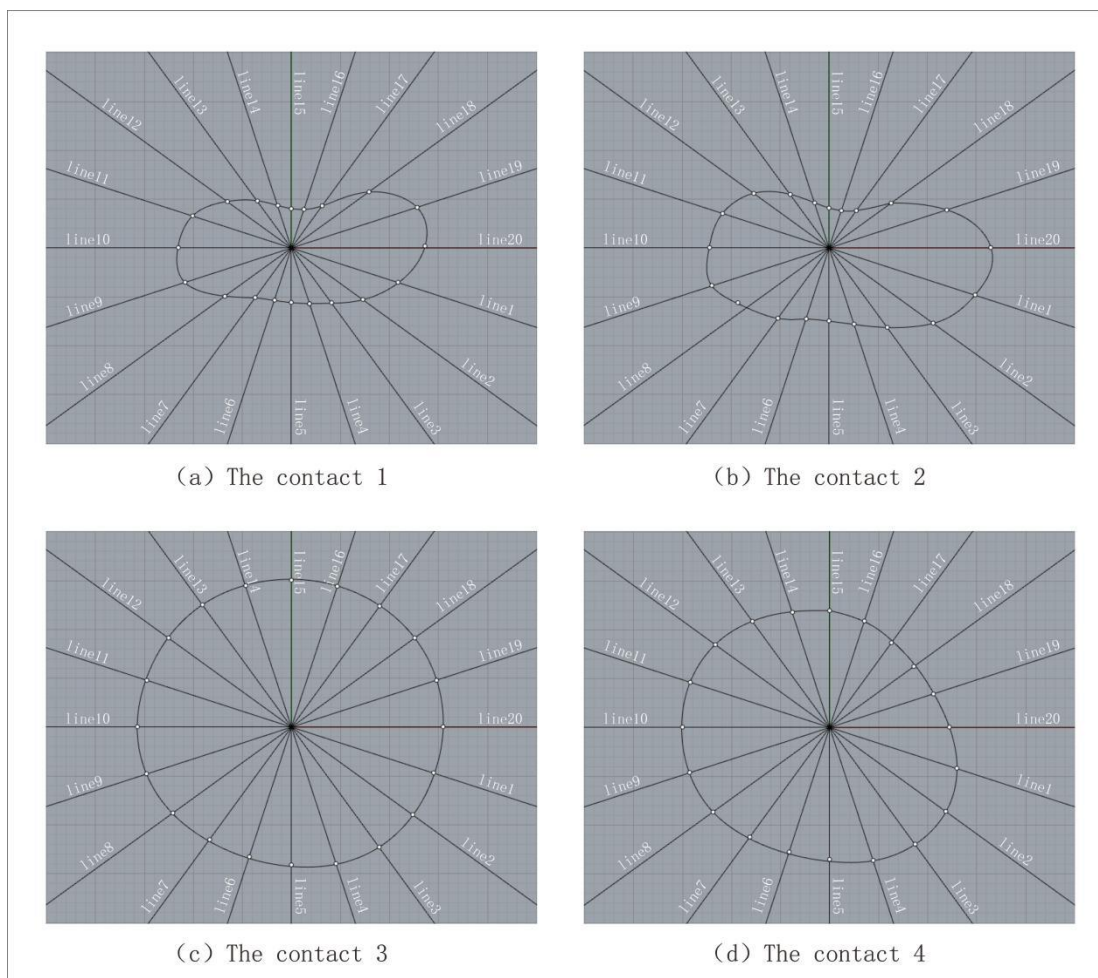


Figure 13: Midline of the profile where the contact is located

Product Optimization and Improvement Design

Functional Role: The metacarpophalangeal joint primarily serves as a supportive platform rather than applying inward compressive pressure on the clay material, unlike Contact Points 1 and 2.

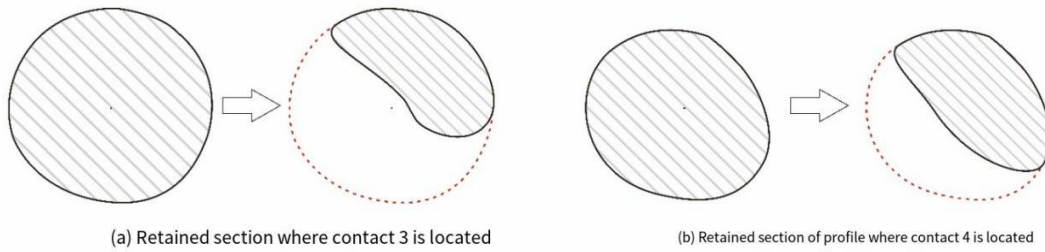


Figure 14: The section where the third and fourth contacts are retained

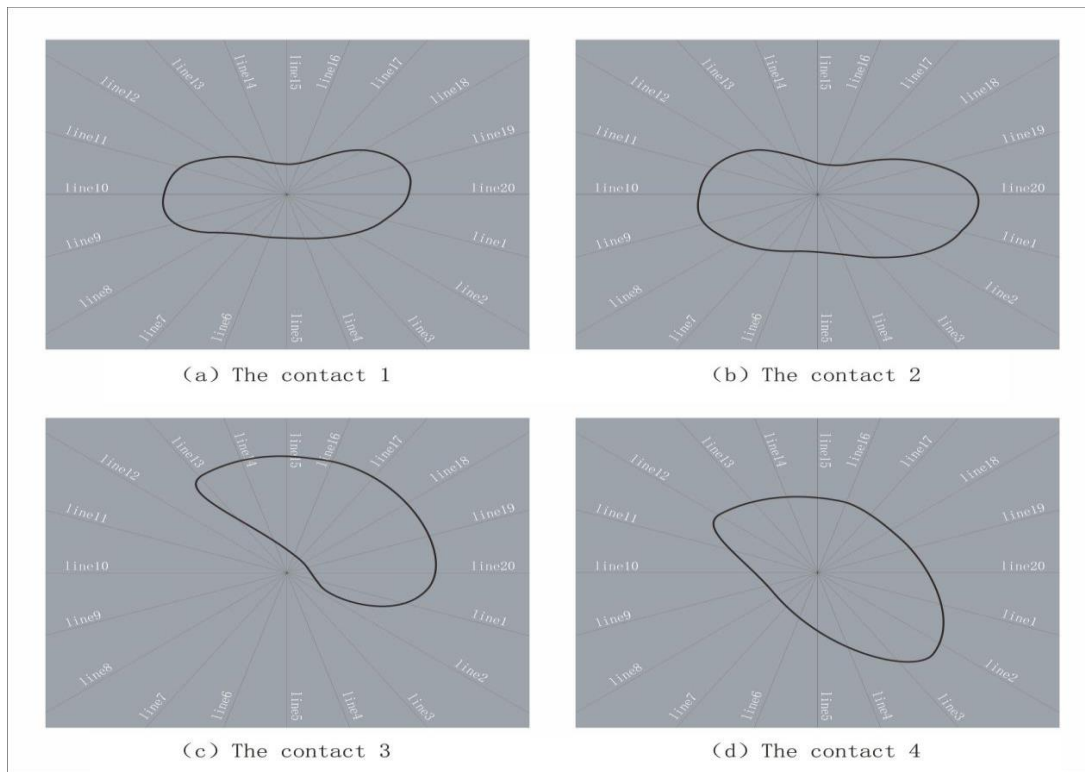


Figure 15: Optimum line of the profile where the contact is located

To ensure scientific rationality of weight distribution, the handle's center of gravity should be precisely aligned with Contact Points 1 and 2. For Contact Points 3 and 4, only structural regions defined by the median path lines corresponding to actual hand contact areas should be retained (Figure 14). This design effectively reduces the handle's tail mass, enhancing operational ease and efficiency. Consequently, the optimal contour lines at contact points (Figure 15) and their corresponding optimal points (Table 9) can be derived.

Table 9: Optimal line coordinates

The best point coordinates of contact 1 in the profile	The best coordinates of contact two in the profile	The best coordinates of contact three in the profile	The best coordinates of contact four in the profile
10.88, 3.54, 75.27	14.89, 4.84, 81.09	5.30, 7.30, 25.81	12.98, 4.22, 56.43
7.284, 5.30, 75.27	10.62, 7.72, 81.09	1.42, 4.36, 25.81	11.85, 8.61, 56.43
4.11, 5.65, 75.27	5.93, 8.16, 81.09	0,3.21, 25.81	8.71, 11.99, 56.43
1.86, 5.73, 75.27	2.54, 7.83, 81.09	0.80, 2.48, 25.81	4.43, 13.64, 56.43

0, 5.61, 75.27	0, 7.50, 81.09	1.38, 1.90, 25.81	0, 13.55, 56.43
1.75, 5.39, 75.27	2.37, 7.29, 81.09	1.87, 1.36, 25.81	4.16, 12.79, 56.43
3.71, 5.11, 75.27	5.26, 7.24, 81.09	2.28, 0.74, 25.81	8.18, 11.27, 56.43
6.82, 4.96, 75.27	9.35, 5.65, 81.09	2.67, 1.42, 25.81	11.94, 8.68, 56.43
10.86, 3.53, 75.27	11.98, 3.89, 81.09	3.28, 1.06, 25.81	14.31, 4.65, 56.43
11.56, 0,75.27	12.24, 0,81.09	12.01, 3.90, 25.81	15.05, 0,56.43
10.11, 3.28, 75.27	10.91, 3.54, 81.09	6.49, 3.50, 25.81	14.25, 4.63, 56.43
6.56, 4.77, 75.27	7.71, 5.60, 81.09	8.32, 9.79, 25.81	11.69, 8.49, 56.43
3.51, 4.83, 75.27	3.99, 5.50, 81.09	9.09, 12.52, 25.81	7.90, 10.88, 56.43
1.41, 4.35, 75.27	1.50, 4.63, 81.09	4.70, 14.47, 25.81	3.83, 11.78, 56.43
0,4.03, 75.27	0,4.10, 81.09	0,15.07, 25.81	0,11.95, 56.43
1.29, 3.96, 75.27	1.24, 3.82, 81.09	4.68, 14.41, 25.81	3.55, 10.92, 56.43
3.13, 4.31, 75.27	2.79, 3.83, 81.09	9.00, 12.39, 25.81	6.31, 8.69, 56.43
8.11, 5.51, 75.27	6.33, 4.60, 81.09	12.57, 9.13, 25.81	8.60, 6.25, 56.43
12.83, 4.17, 75.27	12.03, 3.91, 81.09	14.79, 4.81, 25.81	10.59, 3.44, 56.43
13.64, 0,75.27	16.49, 0,81.09	15.45, 0,25.81	12.22, 0,56.43

RESULTS AND ANALYSIS

Design Input

In the overall handle design, ease of cleaning and minimalist aesthetics were prioritized. While ensuring the handle closely follows the optimal contour lines of hand contact areas, the design emphasizes a streamlined form with soft, flowing curves. This approach not only enhances visual harmony but also facilitates daily cleaning and maintenance. As a low-wear consumable, the carving knife handle boasts a long service life, reducing the need for frequent replacements. Coupled with black pottery artisans' deep passion for ceramic arts and their willingness to invest in high-quality tools, cost considerations were temporarily excluded from primary design constraints.

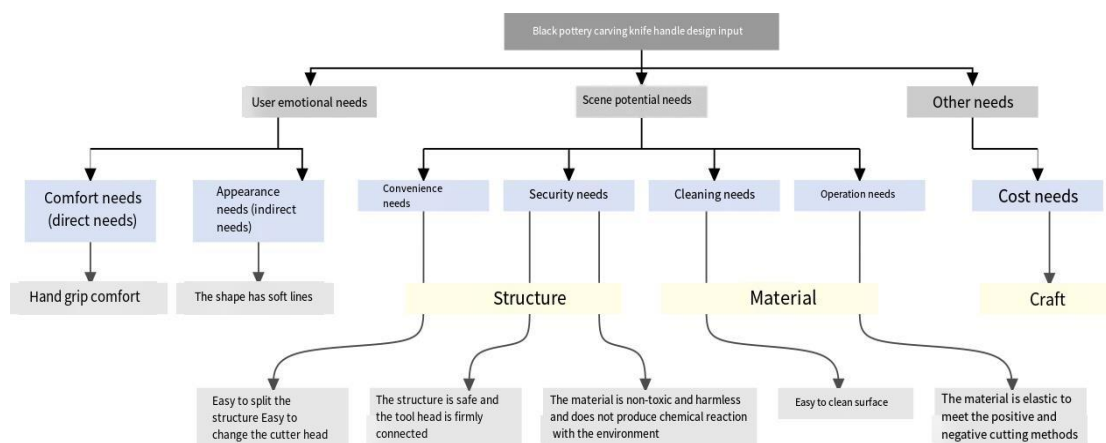


Figure 16: Handle design input

Design Output

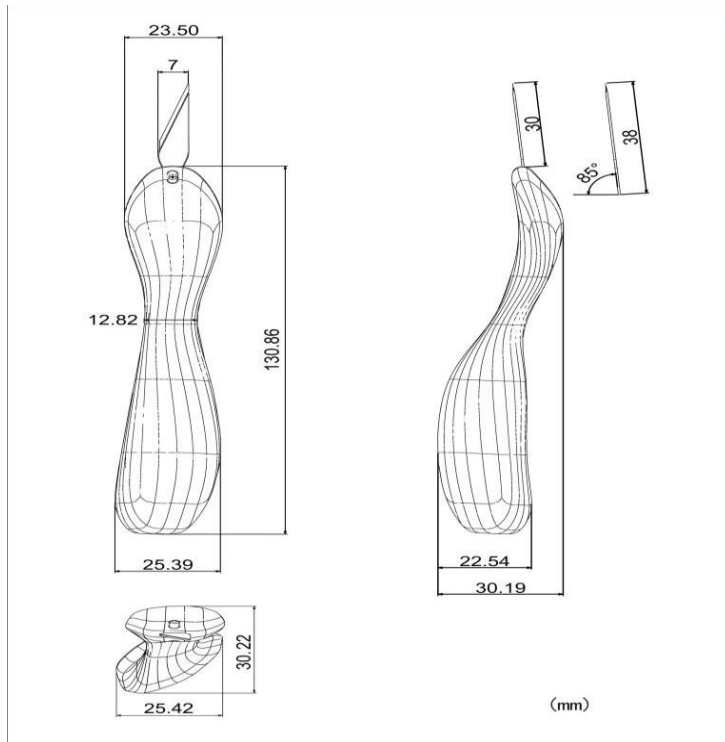


Figure 17: Three product views

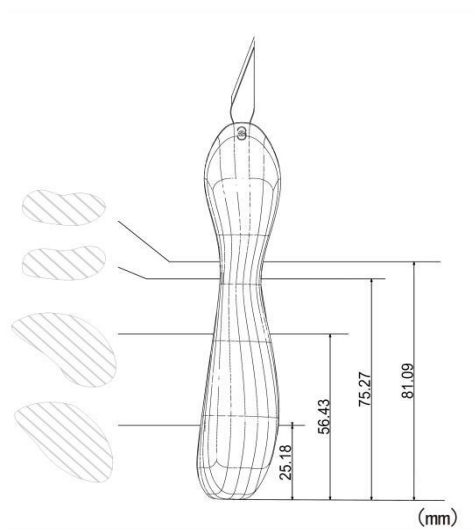


Figure 18: Model and corresponding section

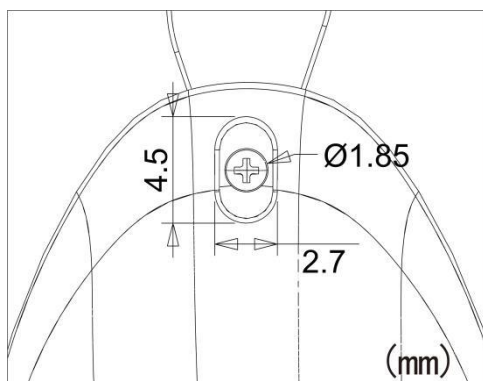


Figure 19: Detail size diagram

The blade and handle are secured via a snap-fit fastening mechanism. A slot inside the handle accommodates the blade, which is further stabilized by two threaded locking structures inserted from both sides. Tightening screws ensures blade stability and safety during use. This design excels in detachability and flexibility, allowing artisans to swap blades of varying lengths or shapes for diverse tasks, thereby enhancing versatility and efficiency. To streamline production and maintenance, standardized blades widely available on the market were selected, simplifying procurement and replacement.

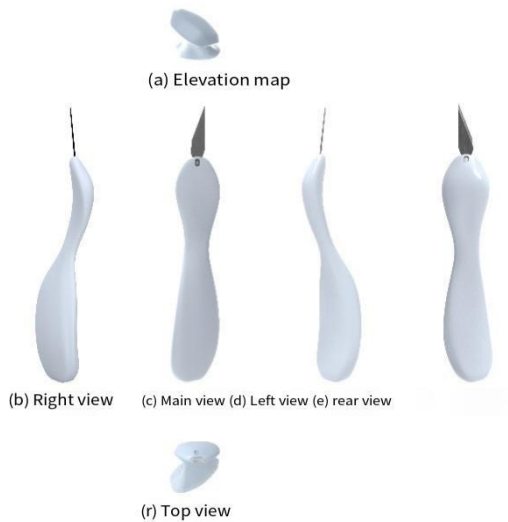


Figure 20: Six views of the product

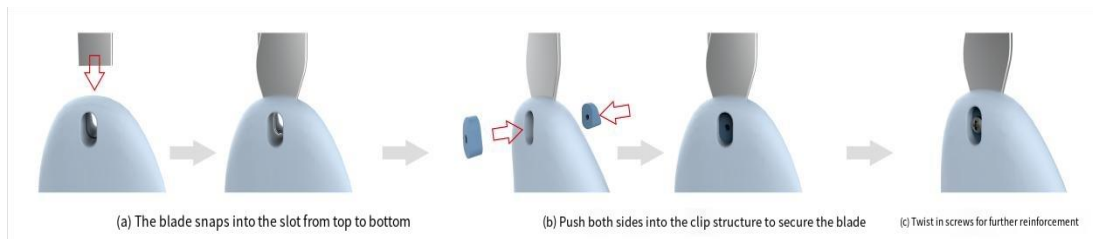


Figure 21: Blade installation procedure diagram

Aesthetic considerations guided the upward curvature above Contact Point 2, aligning with the lower profile's graceful arc to maintain a streamlined appearance. This design also optimizes weight distribution by concentrating mass in the grip area, improving comfort and stability.

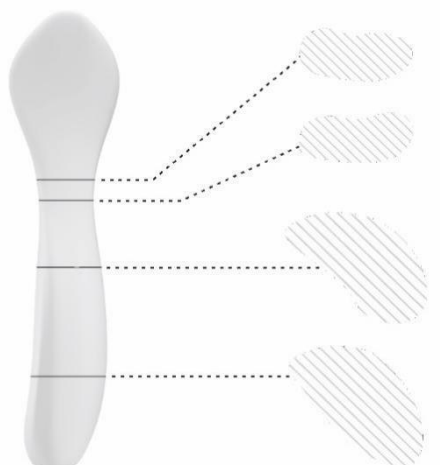


Figure 22: Physical model and corresponding profile

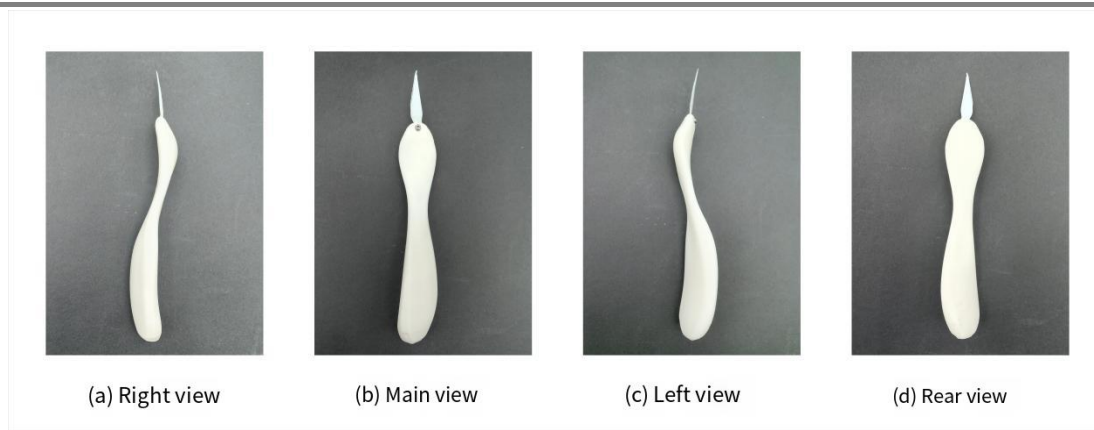


Figure 23: Physical display

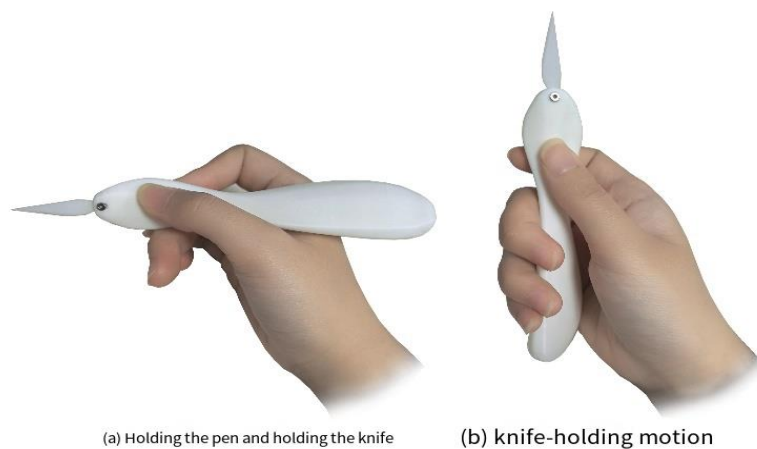


Figure 24: Use scenario simulation display

Design Evaluation

Ten evaluators with ceramic carving expertise tested physical models by simulating pen-holding and handle-holding postures for 15 minutes. Comfort was assessed across five dimensions: pressure distribution, surface ergonomics, rotational ease, cushioning, and long-term grip comfort, scored on a 1–9 scale (1–3: uncomfortable; 4–6: moderately comfortable; 7–9: highly comfortable). Surface ergonomics scored the highest average of 8.4, demonstrating that the optimized handle aligns with natural hand movements during the forward and reverse knife technique. Rotational ease (8.2) and long-term grip comfort (8.1) followed, confirming effortless blade manipulation and reduced fatigue during prolonged carving.

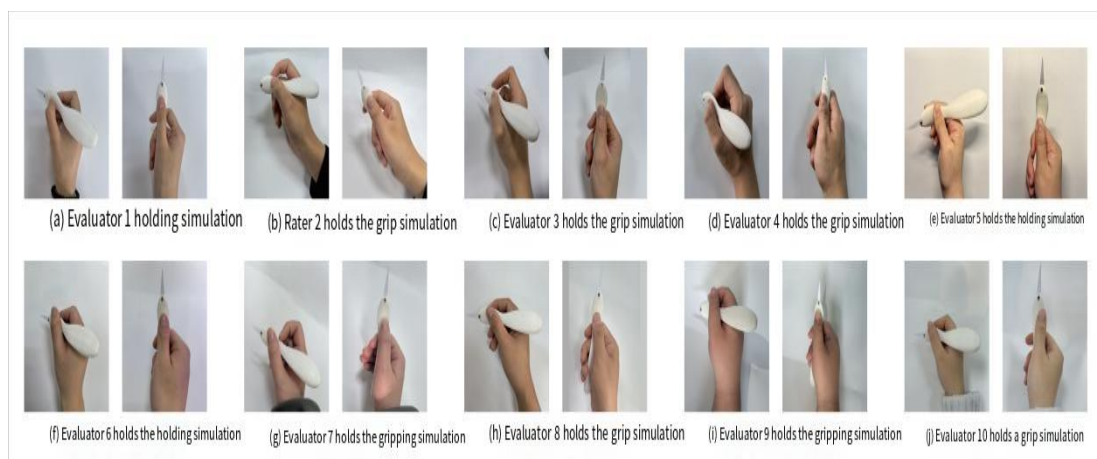


Figure 25: Evaluator holding a physical object simulates sculpting action

Table 10: Design evaluation of holding comfort

project	Evaluator	Hold comfort design evaluation					Average value
		Pressure distribution Comfort	Curved surface comfort	Rotational comfort	Cushioning comfort	Long-lasting comfort	
		Ratings: Uncomfortable 1-3, moderately comfortable 4-6, very comfortable 7-9					
1	Xia	9	9	7	8	8	8.2
2	Li ¹	8	9	8	8	7	8
3	Yan	7	8	8	6	8	7.4
4	Li ²	8	9	9	7	9	8.4
5	Qin	8	8	9	8	9	8.4
6	Zhao	8	9	9	9	8	8.6
7	Zhang	7	8	9	9	8	8.2
8	shen	7	7	8	8	7	7.4
9	Wang	9	9	7	9	8	8.4
10	Qi	9	8	8	8	9	8.4
Average		8.0	8.4	8.2	8.0	8.1	/

While pressure distribution and cushioning scored slightly lower (both 8.0), evaluators emphasized the need for material upgrades. Future iterations will prioritize advanced materials to enhance comfort and user experience.

Material Selection

Material choice critically impacts carving performance. For black pottery's wet-carving process, which demands moderate force, ABS material was selected for its balanced hardness and resilience. While ABS meets current rigidity requirements, future research will explore optimizing elasticity to better align with artisans' needs. Detailed discussions will follow in subsequent publications.

CONCLUSION

This study optimized efficiency and operator comfort for the forward and reverse knife technique in black pottery carving. Key findings include: (1) Surface ergonomics (8.4) confirms superior alignment with hand contours during carving; (2) Rotational ease (8.2) reflects enhanced dynamic ergonomic compatibility; (3) Long-term grip comfort (8.1) demonstrates effective pressure dispersion during extended use; (4) Pressure distribution and cushioning (both 8.0) highlight opportunities for material innovation. These advancements improve artisan comfort, efficiency, and health outcomes while bridging traditional craftsmanship with modern technology.

REFERENCES

1. Basak, T. (2007). Role of various elliptical shapes for efficient microwave processing of materials. *AIChE journal*, 53(6), 1399-1412.
2. Bhaskaran, V. (2024). Designing for Trust: The Crucial Role in Digital User Experiences. *Journal of User Experience*, 19(2), 53-59.
3. Buchczyk, M. (2015). Heterogeneous Craft Communities: Reflections on Folk Pottery in Romania. *Journal of Museum Ethnography*, 8(28), 28-49.
4. Burden, A. G. (2022). Affordances in collaborative robotic production for artisan crafts and hybrid design. *Queensland University of Technology*.
5. Chinyana, B. (2017). An ethnographic study pottery production, decorative styles and functions in relation to prehistoric pottery from Mumbwa caves. *The University of Zambia*.
6. Colomban, P. (2020). Glass, Pottery and enamelled objects: Identification of their technology and origin. *Conservation Science: Heritage Materials*, 2nd Edition, P. Garside & E. Richardson Eds, RSC.
7. Gardner, L., & Chan, T. M. (2007). Cross-section classification of elliptical hollow sections. *Steel and Composite Structures*, 7(3), 185.
8. Hassenzahl, M. (2013). User experience and experience design. *The encyclopedia of human-computer interaction*, 2, 1-14.
9. Jędrych, M., Gorzkiewicz, D., Deja, M., & Chodnicki, M. (2025). Application of 3D scanning and computer simulation techniques to assess the shape accuracy of welded components. *The International Journal of Advanced Manufacturing Technology*, 138(1), 127-135.
10. Pätöprstý, B., Vozár, M., Hrušecký, R., & Buranský, I. (2024). Comparison of optical 3D scanner and coordinate measurement system from the standpoint of macro-geometry measurement. *Journal of Measurements in Engineering*, 12(1), 99-107.
11. Vickers, M. (1985). Artful crafts: the influence of metalwork on Athenian painted pottery. *The Journal of Hellenic Studies*, 105, 108-128.
12. Yussif, I., Adu-Gyamfi, V., & Tabi-Agyei, E. (2018). Documentation of some identified traditional pottery decorative techniques in Northern Ghana. *Asian Research Journal of Arts & Social Sciences*, 6(3), 1-11.